Tellus (1990), *42A*, 557–567

Numerical studies of the surface-wave effects on the upper turbulent layer in the ocean

By LE NGOC LY, *Institute for Naval Oceanography, Stennis Space Center, Mississippi 39529, USA*

(Manuscript received 21 March 1989; in final form 16 October 1989)

ABSTRACT

The surface-wave effects on the structure of the ocean boundary layer are studied with a numerical boundary-layer model which consists of a closed system of equations for momentum, turbulent kinetic energy, turbulent exchange coefficient and expression for ocean stratification. Boundary conditions at the air–sea interface are calculated by use of a coupled air–sea boundary-layer model. The surface-wave effect is described by discontinuities of turbulent kinetic energy flux and mean wind energy flux across the air–sea interface. A series of numerical experiments is carried out to determine the effects of surface waves on the structure of the upper turbulent layer in the ocean. The numerical simulations demonstrate that surface waves strongly reduce a part of mean wind energy flux transmitted to the drift current and the current magnitude. These characteristics are strongly dependent on surface heat flux. The surface waves also reduce the neutral drag coefficient for a given wind speed to better match observations, but waves strongly increase turbulent kinetic energy at the ocean surface. The computations also confirm that the ratio of the mean wind energy flux transmitted to the drift current, to the total mean wind energy flux transmitted to the ocean is weakly dependent on surface heat flux. The model results are compared with observed data where available.

1. Introduction

The study of the upper turbulent layer structure in the ocean is one of the important problems of ocean physics. The transport of momentum, heat, humidity and salt occurs across the air–sea interface. The character of this transport is regulated by the turbulence of the air–sea boundary layers. Turbulent activity in the upper layer of the ocean depends on the vertical gradients of velocity and density which, in turn, affect the turbulent processes in the upper ocean. The turbulence structure in the upper layer of the ocean has a strong influence on the dynamics of the ocean. Therefore modeling the structure of the upper turbulent layer is important not only in theoretical problems, but also in many applied oceanography problems.

One of the main differences between a solid surface and water surface is that a solid surface remains stationary, while surface waves are generated and maintained by surface wind stress. Propagating surface waves interact with wind to produce perturbations in Reynolds fluxes and wind velocity. Turbulent motion in the surface layer of the ocean is strongly influenced by the wind. This influence leads to the formation of surface waves, drift currents and turbulent motions of various scales, tending to increase vertical mixing in the surface layer of the ocean.

Influences of surface waves on surface layers of the atmosphere and ocean have been well noted by Geernaert et al. (1988), Dubov (1974), Kitaigorodski (1973), Lai and Shemdim (1971), and Roll (1965). These influences are very complex and still poorly understood, although there have been numerous experimental investigations and analytical studies. There is not sufficient observational data to specify the quantitative impact of surface waves on characteristics of air–sea boundary layers.

One of the major difficulties in air–sea interaction problems is the correct description of surface-wave effects. Here, the distinctive feature is the oscillation of the air–water interface, so that the standard methods of the Eulerian description of turbulence are generally inapplicable. The influence of surface waves on the dynamics of turbulent exchange in the surface layer of the ocean must be taken into account while formulating boundary conditions at the upper boundary of the mixing layer in the ocean.

The traditional approach in treating surface waves in physical oceanography is by expressing the direct influence of the surface wind waves by the roughness length z_0. This roughness length is usually related to such particular characteristics of the local surface waves as phase velocity, height and wave slope. It is customary to assume continuity of various physical characteristics across the air–sea interface. Some studies (Klein and Coantic, 1981; Kundu, 1980) simply used the turbulent kinetic energy flux from the atmosphere associated with surface waves as a boundary condition in ocean boundary-layer models.

In this study we examine, by use of a numerical model, surface-wave effects on the properties of the oceanic boundary layer. The conditions on the air–water interface are obtained from the solution to the problem of coupled air–sea boundary layers (Ly, 1986). The specific properties studied are turbulent kinetic energy, drag coefficient, and surface drift current. This study emphasizes the wind energy flux transmitted to surface waves, to the drift current and their ratio to total mean wind energy flux transmitted to the ocean. In Section 2, the problem for the oceanic planetary boundary layer is formulated. In Section 3, the numerical results and some comparisons with observations, where available, are given. And finally, the conclusions and remarks of the study are given in Section 4.

2. Basic equations and boundary conditions including ocean surface-wave effects

It is assumed that stationary and horizontally homogeneous conditions exist for ocean boundary-layer flows. Governing equations describing the oceanic boundary-layer flow include the equations of motion, turbulent kinetic energy (TKE), turbulent exchange coefficient (TEC), and expressions for stratification. The energy transferred across the air–sea interface is taken into account by the method of bulk parameterization.

2.1. Governing equations

The equations of motion in Cartesian form describing the oceanic planetary boundary-layer flow can be written as (Yeh, 1974)

$$\frac{\mathrm{d}}{\mathrm{d}z} K \frac{\mathrm{d}u}{\mathrm{d}z} + fv = \frac{1}{\rho}\frac{\partial p}{\partial x}, \quad \frac{\mathrm{d}}{\mathrm{d}z} K \frac{\mathrm{d}v}{\mathrm{d}z} - fu = \frac{1}{\rho}\frac{\partial p}{\partial y}, \tag{1}$$

where x, y, and z are coordinates such that the x-axis is in the direction of the surface wind vector and the z-axis is taken to be perpendicular to the interface, with the positive direction downward for the ocean. The fluid velocity components are u and v. The Coriolis parameter is denoted by f, and the vertical turbulent exchange coefficient is K. The density of seawater is denoted by ρ, and pressure is denoted as p. The subscript 0 denotes either the reference value for ρ_0, or surface values for roughness length z_0.

The turbulent exchange coefficient, K, is determined from the turbulent kinetic energy, E, and length scale, l, by the Prandtl–Kolmogorov hypothesis (Monin, 1986) as

$$K = l E^{1/2}. \tag{2}$$

The length scale, l, can be determined by the modified von Karman's formula (Monin, 1986)

$$l = -2kc^{1/4}\phi/(\mathrm{d}\phi/\mathrm{d}z), \tag{3}$$

where

$$\phi = \left(\frac{\mathrm{d}u}{\mathrm{d}z}\right)^2 + \left(\frac{\mathrm{d}v}{\mathrm{d}z}\right)^2 - \frac{g}{\rho_0}\frac{\mathrm{d}\rho}{\mathrm{d}z}. \tag{4}$$

The constant c is taken equal to 0.046 and k is von Karman's constant (taken as 0.4). Using (2), (3) and (4), the turbulent exchange coefficient K can be expressed in terms of TKE, E, by the following equation (Ly and Takle, 1988)

$$K = E\left(\frac{K_0}{E_0} + kc^{1/4}\int_{z_0}^{z}\frac{\mathrm{d}z}{E^{1/2}}\right), \tag{5}$$

where K_0 and E_0 are, respectively, TEC and TKE at roughness length $z = z_0$.

Turbulent kinetic energy, E, is determined from the budget equation for TKE

$$K\left[\left(\frac{du}{dz}\right)^2+\left(\frac{dv}{dz}\right)^2-\frac{g}{\rho_0}\frac{d\rho}{dz}\right] + \alpha_e\frac{d}{dz}K\frac{dE}{dz}-c\frac{E^2}{K}=0. \tag{6}$$

The first two terms on the left-hand side represent shear production, and the third represents buoyant production due to vertical gradients of seawater density (where ρ_0 and ρ are the mean and local values of density, g is the gravitational acceleration). The fourth term is the diffusion of TKE at the rate $\alpha_e K$, where α_e is a constant ($\alpha_e = 0.73$). The last term is the dissipation of TKE, where c is the same constant as in (4) and (6) ($c = 0.046$) (see Zilitinkevich, 1970). The Prandtl number is assumed to be unity for both the atmosphere and ocean.

The system of eqs. (1), (2), (5), and (6) will be closed by introducing an equation for density gradients in the ocean boundary layer. To simplify modeling the structure of the upper ocean layer and to focus attention on the study of the effects of surface waves, approximate formulas for the vertical gradients of seawater density have been employed.

For the oceanic boundary, the vertical distribution of seawater density is approximated by the formula (Ly, 1981)

$$\frac{d\rho}{dz}=\tilde{A}\rho\times\delta(z-z_c)+(\Gamma_1-\Gamma_2)\times\sigma(z-z_c)+\Gamma_2, \tag{7}$$

where $\delta(z-z_c)$ is the Dirac delta function and

$$\sigma(z-z_c)=\begin{cases}0, & \text{if } 0\leqslant z\leqslant z_c\\ 1, & \text{if } z>z_c,\end{cases}$$

where $\tilde{A}$ is a characteristic magnitude of the jump in seawater density, z_c is the depth of the density-jump layer (Kamenkovich and Monin, 1978), $\sigma(z-z_c)$ is the unit function, and Γ_1 and Γ_2 are the vertical gradients of seawater density in the water layer lying, respectively, below and above the density-jump layer. The analytic expression for density in (7) specifies that the upper layer of the ocean is well mixed and is bounded below by a highly stable layer. Values for $\tilde{A}$, Γ_1, Γ_2, and z_c used in the simulations are typical values taken from observed data (see Section 3).

By denoting the vertical fluxes of horizontal momentum as

$$\tau_x=K\frac{du}{dz},\quad \tau_y=K\frac{dv}{dz}, \tag{8}$$

then eqs. (1) and (6) can be written in the form

$$\frac{d^2\tau_x}{dz^2}+f\frac{\tau_y}{K}=0,\quad \frac{d^2\tau_y}{dz^2}-f\frac{\tau_x}{K}=0, \tag{9}$$

$$\frac{\tau_x^2+\tau_y^2}{K}-K\frac{g}{\rho_0}\frac{d\rho}{dz}-c\frac{E^2}{K}+\alpha_e\frac{d}{dz}K\frac{dE}{dz}=0. \tag{10}$$

To model the vertical turbulent structure of the upper ocean layer, the atmospheric boundary layer is considered only to obtain a correct condition at the air–sea interface. Hereafter subscript $i = 1$ represents characteristics in the atmospheric boundary layer and $i = 2$ represents those in the ocean.

The boundary conditions at the air–sea interface for problems of air–sea interaction and of ocean dynamics are characterized by the air–sea interface oscillating vertically around a certain mean position. Therefore, the concept of a surface-wave layer is introduced. Physically, the wave layer can augment or decrease momentum transfer due to increased surface area, foam, spray, slope of the wave field. The particular feature of the wave layer is that physical processes of this layer cannot be described by the equations of the type (1)–(6) (Ly, 1986). The thickness of the wave layer is small (of order of the magnitude of the surface-wave height) in comparison with boundary-layer depths of the atmosphere and ocean. It is assumed that in the steady-state condition the momentum transfer and the y-component of velocity are continuous across the wave layer (traditional boundary conditions), i.e.,

$$\left(K_1\rho_1\frac{du_1}{dz_1}\right)\Big|_{z_{01}}=-\left(K_2\rho_2\frac{du_2}{dz_2}\right)\Big|_{z_{02}},$$
$$\left(K_1\rho_1\frac{dv_1}{dz_1}\right)\Big|_{z_{01}}=-\left(K_2\rho_2\frac{dv_2}{dz_2}\right)\Big|_{z_{02}} \tag{11}$$

$$v_1(z_1)|_{z_{01}}=v_2(z_2)|_{z_{02}}, \tag{12}$$

where z_{01} and z_{02} are the roughness length of the upper and lower boundaries of the wave layer.

Based on conservation of energy and dimensional analysis, the equation for turbulent kinetic energy flux can be written as

$$\left(K_1\,\rho_1\,\frac{dE_1}{dz_1}\right)\bigg|_{z_{01}} + \left(K_2\,\rho_2\,\frac{dE_2}{dz_2}\right)\bigg|_{z_{02}} = C_1\,\rho_1\,u_{*1}^3, \tag{13}$$

where C_1 must be understood as a non-dimensional parameter representing the surface wind wave effect and each value of C_1 is matched to a marine surface state in the air–sea interface; u_{*1} is friction velocity of air flow. Similar reasoning leads to an equation for the mean wind energy flux transferred to the water:

$$\left(K_1\,\rho_1\,\frac{du_1}{dz_1}\,u_1\right)\bigg|_{z_{01}} + \left(K_2\,\rho_2\,\frac{du_2}{dz_2}\,u_2\right)\bigg|_{z_{02}} = C_1\,\rho_1\,u_{*1}^3. \tag{14}$$

Eqs. (13) and (14) show that the turbulent kinetic energy flux and mean wind energy flux have a discontinuity between air and water, and that not all the energy is transmitted to the drift current, but a part goes to generate and maintain the surface waves ($C_1\,\rho_1\,u_{*1}^3$). It is worth noting that $C_1 = 0$ gives the traditional conditions of continuity for the physical characteristics across the interface.

The roughness length z_{01} can be written in the Charnock form (Charnock, 1955)

$$z_{01} = \frac{u_{*1}^2}{g}\,b\left(\frac{\rho_1}{\rho_2}\right), \tag{15}$$

where the factor $b(\rho_1/\rho_2)$ can be taken as an empirical constant equal to 0.05 (Kitaigorodski, 1973). Note that b may also depend on wave slope (Geernaert, 1988).

It is observed that near the surface shear production and dissipation are the main components in the turbulent kinetic energy budget for both the atmosphere and ocean. Then the boundary conditions for the turbulent kinetic energy at the air–sea interface can be written in the general form (Ly, 1989)

$$E(z)|_{z_0} = \gamma u_*^2, \tag{16}$$

where γ is a non-dimensional parameter to be determined. By use of (6), (13), (14), and (16), we have the following equation for calculating γ from the given surface-wave parameter C_1 (Ly, 1989).

$$\left(\frac{c\gamma}{\alpha_e}\right)^{1/2}\left(\frac{1}{c\gamma} - \gamma\right)\left[1 + \left(\frac{\rho_1}{\rho_2}\right)^{1/2}\right] = C_1. \tag{17}$$

If $C_1 = 0$ in (17), γ is equal to $c^{-1/2}$ then (16) can be written in the following form

$$E(z)|_{z_0} = c^{-1/2}u_*^2. \tag{18}$$

Eq. (18) is a traditional boundary condition for the turbulent kinetic energy at the surface in the atmospheric boundary-layer over land (for $i = 1$) (Monin and Yaglom, 1971) and air–sea boundary layer problems (Ly, 1989).

At the boundaries away from the air–sea interface, wind-induced currents tend toward geostrophic currents, and the momentum flux and the turbulent kinetic energy tend toward zero:

$$u(z)|_{z_\infty} \to u_g, \quad v(z)|_{z_\infty} \to v_g, \tag{19}$$

$$K\frac{du}{dz}\bigg|_{z_\infty} \to 0, \quad K\frac{dv}{dz}\bigg|_{z_\infty} \to 0, \quad E(z)|_{z_\infty} \to 0. \tag{20}$$

By use of (8), boundary conditions (11) and (20) can be written in terms of the vertical turbulent fluxes as follows:

at $z \to z_0$:

$$\tau_x(z)|_{z_0} \to u_*^2, \quad \tau_y(z)|_{z_0} \to 0, \tag{21}$$

at $z \to z_\infty$:

$$\tau_x(z)|_{z_\infty} = \tau_y(z)|_{z_\infty} \to 0, \quad E(z)|_{z_\infty} \to 0. \tag{22}$$

2.2. *Non-dimensional equations and boundary conditions*

For convenience, the problem is solved in non-dimensional form. Equations are non-dimensionalized by setting

$$u_n = -(k/u_*)\,u, \quad v_n = -(k/u_*)\,v,$$
$$z_n = fz/(ku_*) = z/\Omega, \quad E_n = c^{1/2}E/u_*^2,$$
$$K_n = K/(ku_*\,\Omega), \quad \tau_{xn} = -\tau_x/u_*^2, \quad \tau_{yn} = -\tau_y/u_*^2, \tag{23}$$

where $\Omega = ku_*/f$ is about the order of the planetary boundary layer thickness and c is an empirical non-dimensional constant (0.046). The system of equations and boundary conditions with the transformations given by (23) are written in non-dimensional form (the subscript n hereafter indicates any quantity in non-dimensional form) as follows:

$$\frac{\mathrm{d}^2 \tau_{xn}}{\mathrm{d}z_n^2} + \frac{\tau_{yn}}{K_n} = 0, \quad \frac{\mathrm{d}^2 \tau_{yn}}{\mathrm{d}z_n^2} - \frac{\tau_{xn}}{K_n} = 0, \tag{24}$$

$$\frac{\tau_{xn}^2 + \tau_{yn}^2}{K_n} - K_n R_n - \frac{E_n^2}{K_n} + v_0 \frac{\mathrm{d}}{\mathrm{d}z_n} K_n \frac{E_n}{\mathrm{d}z_n} = 0, \tag{25}$$

$$K_n = E_n \left(\frac{K_{0n}}{E_{0n}} + \int_{z_{0n}}^{z_n} \frac{\mathrm{d}z_n}{E_n^{1/2}} \right), \tag{26}$$

where K_{0n} and E_{0n} are the non-dimensional turbulent exchange coefficient and turbulent kinetic energy, respectively, at roughness length z_{0n}.

$$R_n = \frac{k^4}{f} \frac{g}{\rho_0} \left(\frac{\Delta\rho}{\pi} \frac{m}{1+a^2} \frac{\Gamma_1 - \Gamma_2}{\pi} \tan^{-1} a + \frac{\Gamma_1 + \Gamma_2}{2} \right), \tag{27}$$

where $a = m(z_n - z_{nc})$;

$$\mu = -\frac{g}{\theta_{01}} \frac{k^2 Q_{01}}{\rho_1 c_p f u_{*1}^2}; \tag{28}$$

μ is a non-dimensional surface heat flux that is used to specify the surface stability (Tennekes, 1973); $\Delta\rho_2$ is the difference in seawater density between the upper and lower boundaries of the density-jump layer in the ocean; m is a parameter controlling the shape of the seawater density both in the shape of the jump layer and in the matching between the two regions of constant gradient; v_0 and π are constants ($v_0 = 0.54$ and $\pi = 3.1416$); Q_{01} is the surface heat flux; θ_{01} and ρ_0 are the basic state temperatures and densities of the atmosphere and the ocean, respectively. A μ value of -100 corresponds to the surface heat flux about 500 W/m^2 (Ly and Takle, 1988).

By use of (18) and (21), surface boundary conditions for non-dimensional momentum fluxes and turbulent kinetic energy can be written as

$$\tau_{xn}(z_n)|_{z_{0n}} = 1, \quad \tau_{yn}(z_n)|_{z_{0n}} = 0, \quad E_n(z_n)|_{z_{0n}} = c^{1/2}\gamma, \tag{29}$$

where γ is calculated from (17).

At the boundaries away from the interface, the non-dimensional momentum fluxes and turbulent kinetic energy have the following form

$$\tau_{xn}(z_n)|_{z_{\infty n}} = \tau_{yn}(z_n)|_{z_{\infty n}} \to 0, \quad E_n(z_n)|_{z_{\infty n}} \to 0. \tag{30}$$

From the conditions for velocities at the ocean surface follow the expressions for the geostrophic drag coefficient (C_{Dg}) and angle (α_1) between the vectors of surface stress and the geostrophic wind

$$C_{\mathrm{Dg}}^2 = \left(\frac{u_{*1}}{kU_{\mathrm{g1}}} \right)^2 = \frac{[1 - 2m_0 \cos\beta + m_0^2 + A + (kC_1 C_{\mathrm{Dg}})^2]}{M_1^2 + M_2^2}, \tag{31}$$

$$\tan\alpha_1 = -\frac{1 - m_0(M_0 \sin\beta + \cos\beta) - C_{\mathrm{Dg}} k C_1/\cos\alpha_1}{M_0 - m_0(\cos\beta - M_0 \sin\beta)}, \tag{32}$$

where

$$A = 2kC_1 C_{\mathrm{Dg}}(m_0 \cos\alpha_2 - \cos\alpha_1), \tag{33}$$

$$m_0 = \frac{U_{\mathrm{g2}}}{U_{\mathrm{g1}}}, \quad \beta - 360° = \alpha_2 - \alpha_1, \quad \left(\frac{\rho_1}{\rho_2} \right)^{1/2} \simeq \frac{1}{28}. \tag{34}$$

β is the angle between the geostrophic wind and geostrophic current

$$M_1 = \left[\frac{\mathrm{d}\tau_{xn1}}{\mathrm{d}z_{n1}} + \left(\frac{\rho_1}{\rho_2} \right)^{1/2} \frac{\mathrm{d}\tau_{xn2}}{\mathrm{d}z_{n2}} \right] \Bigg|_{z_{0n}}, \tag{35}$$

$$M_2 = \left[\frac{\mathrm{d}\tau_{yn1}}{\mathrm{d}z_{n1}} + \left(\frac{\rho_1}{\rho_2} \right)^{1/2} \frac{\mathrm{d}\tau_{yn2}}{\mathrm{d}z_{n2}} \right] \Bigg|_{z_{0n}}, \tag{36}$$

$$M_0 = M_1/M_2. \tag{37}$$

It should be noted that the parameter C_1 representing the surface-wave effect is present in both (31) and (32) and, through these, affects the structure of the oceanic boundary layers.

Eqs. (24)–(30) are solved numerically by a finite-difference method. Eqs. (24) and (25) with the boundary conditions are solved by matrix pivotal-condensation and simple pivotal-condensation methods, respectively. The procedure and algorithm for solving the formulated problem can be found in Ly (1989).

3. The numerical results

Numerical simulations have been carried out for various surface-wave parameters C_1, and surface heat fluxes, μ. The condition on the upper boundary of the ocean boundary layer is obtained from the solution to the problem of coupled air–sea boundary layers. The "external parameters" of the coupled model are taken to be geostrophic wind $U_{g1} = 5$, 10, 15, and 20 m s^{-1}, the ratio between geostrophic wind (U_{g1}) and current (U_{g2}) equal to 0.02, the angle between U_{g1} and U_{g2} equal to $\pi/4$ (Ly, 1989), and latitude equal to 45°. The typical values of stratification of the atmosphere (non-dimensional surface heat flux), μ, are considered to range from -100 to 100 (see Tennekes, 1973). Typical seawater density gradients are chosen to be $\Gamma_1 = 10^{-3}$ kg m^{-4}, $\Gamma_2 = 6 \times 10^{-3}$ kg m^{-4}, and a typical drop of density $\Delta\rho_2 = 1.7$ kg m^{-3}. All "external parameters" of the model could be easily calculated from standard hydrometeorological fields.

The results of the simulations are plotted in Figs. 1–7. We start by examining the model results for friction velocity and roughness length

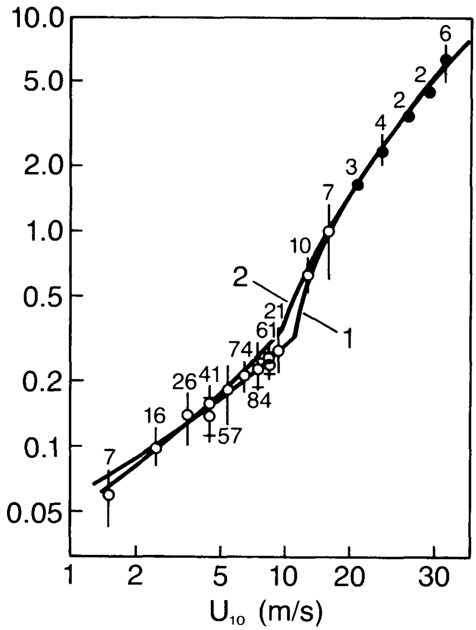

Fig. 1. The friction velocity, u_{*1}, as a function of the 10 m height windspeed, U_{10}. Numbers near the circles indicate the sample size. The vertical lines give the standard deviations from the mean value for u_{*1}. Two dots are given for large samples. Standard deviations corresponding to the later case are marked by horizontal marks on the vertical lines. Curve 1 is from Myers (1959) and Kuznetsov (1970) (after Kitaigorodski, 1973). Curve 2 is the model result for $C_1 = 0$ and zero dimensionless surface heat flux ($\mu = 0$).

in the atmosphere for the case with $C_1 = 0$. Fig. 1 shows results of a number of measurements of friction velocity in the atmosphere, u_{*1} for zero surface heat flux ($\mu = 0$) by Myers (1959) and Kuznetsov (1970) (after Kitaigorodski, 1973) as a function of the wind velocity at the 10 m height above the ocean surface with $C_1 = 0$. The values computed by use of the air–sea coupled model, shown by the curve labeled 2, are in excellent agreement with the measurements over the whole range of wind velocities. The model results show that friction velocity u_{*1} is not sensitive to variations in C_1. The friction velocity, u_{*1}, depends strongly on the 10 m height wind velocity, U_{10}. It is interesting to note that a "knee" of the curve occurs at a 10 m height wind in the range of 10 m s^{-1} to 15 m s^{-1}. This probably results from differences in the mechanism of the momentum transfer for moderate versus strong winds (storm winds). It bears further study since the observations also suggest a kink near these conditions.

Fig. 2 is a plot of surface roughness, z_0, as a function of friction velocity, u_{*1}, under a neutral atmosphere with condition $C_1 = 0$. The figure shows that the roughness parameter varies very widely, from 10^{-5} cm to 10 cm. Therefore, the assumption of a single characteristic value for the roughness parameter of the ocean is unfounded. The lack of agreement of the curves in Fig. 2 is the result of different authors (each with their

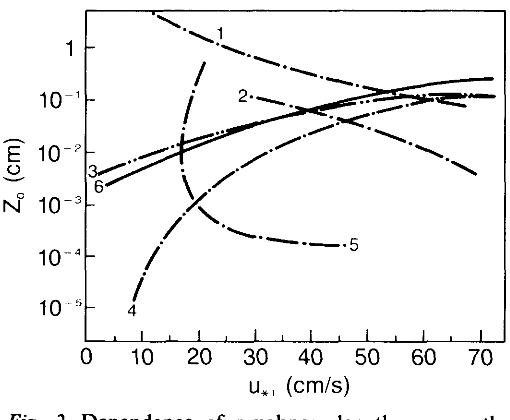

Fig. 2. Dependence of roughness length, z_0, on the friction velocity, u_{*1}, according to (after Kitaigorodski, 1973): (1) Francis (1953); (2) Goptarev (1957); (3) Neumann (1956); (4) Kuznetsov (1963); (5) Deacon and Webb (1962); (6) This model for $C_1 = 0$.

own observations and suggesting their own relationship between roughness length and friction velocity) having different views on the concept of the roughness length and its dependence on atmospheric stratification and ocean-surface state (Kitaigorodski, 1973). The model results given by the curve labeled 6 compare well with the result of Deacon and Webb (1962) over the entire range of friction velocities and suggest a much weaker dependence of roughness length on friction velocity than other authors contend. It is worth noting that, as is the case with the friction velocity, the surface roughness is not sensitive to variations in C_1.

Fig. 3 is a summary of recently published values of drag coefficient for a neutral atmosphere as a function of wind speed at the 10 m height [after Geernaert et al. (1986)] compared with the model drag coefficient. The differences between the drag coefficient are thought to be most likely due to sea states that consistently differ between the measurement sites. It is seen from Fig. 3 that although there is a discrepancy between various curves, the drag coefficient of all investigators increases with the increase of wind speed at the 10 m height for the entire range of the wind velocity (except curve 2 by Large and Pond (1981) for wind speed smaller than 10 m s^{-1}). In this figure, the least discrepancy between

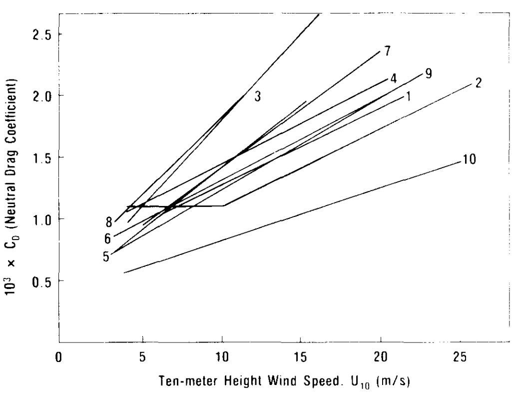

Fig. 3. The published neutral drag coefficient, C_D, as a function of the 10 m height windspeed, U_{10}, according to (after Geernaert et al., 1986): (1) Smith (1980); (2) Large and Pond (1981); (3) Donelan (1982); (4) Garratt (1977); (5) Sheppard et al. (1972); (6) Smith and Banke (1975); (7) Geernaert et al. (1986); (8) This model for $C_1 = 0$; (9) This model for $C_1 = 5$; (10) This model for $C_1 = 10$.

the results of various investigators occurs at low windspeeds (less than 10 m s^{-1}) where the drag coefficient varies from 0.73×10^{-3} to 1.75×10^{-3}. As the windspeed increases from 10 m s^{-1}, these curves tend to diverge, and the drag coefficient varies from 1.2×10^{-3} to 2.5×10^{-3}. It is difficult to explain the change of drag coefficient under strong winds (storm winds). However under storm winds, sprays from the crest waves participate in the momentum exchange (Dubov, 1974), a mechanism still poorly studied and understood. The model drag coefficient for $C_1 = 0$ is shown by curve 8 and is very close to that of curve 3 (Donelan, 1982) for the entire range of wind speeds. Model results of drag coefficient for the surface waves cases of $C_1 = 5$ and $C_1 = 10$ are shown by curves 9 and 10, respectively. It is seen from these that the effect of surface waves is to reduce the drag coefficient for given wind speed. This reduction of drag coefficient is greater for higher wind speeds. The model result for $C_1 = 5$ is in excellent agreement with curve 1 (Smith, 1980) and curve 6 (Smith and Banke, 1975) over the entire range of wind speed. The model result for $C_1 = 10$ shows lower values of the drag coefficient compared to the curves of Fig. 3. This suggests that energy transfer to the waves as computed from $C_1 = 5$ is more realistic than for $C_1 = 10$.

Fig. 4 shows the distribution of total turbulent kinetic energy in the ocean boundary layer for three different values of dimensionless surface heat flux ($\mu = 0$, -100, 100) and of the wave parameter ($C_1 = 20$, 10, and 0) versus dimensionless depth of the ocean. It may be seen from the figure that surface waves have a strong effect on the distribution of total turbulent kinetic energy in the upper part of the ocean boundary layer while, by contrast, the dimensionless surface heat flux has almost none. Here, each line (1, 2, and 3) corresponds to the three values of the dimensionless surface heat flux ($\mu = -100$, 0, and 100), respectively. The effect of surface waves on the distribution of the turbulent kinetic energy in the ocean decreases rapidly with increasing ocean depth. At the "non-stirred level", the seawater turbulent flows are essentially the same as flows with no surface waves, so interaction between the waves and turbulence practically may be ignored. This figure also shows that the surface waves are an additional source of turbulence in the upper

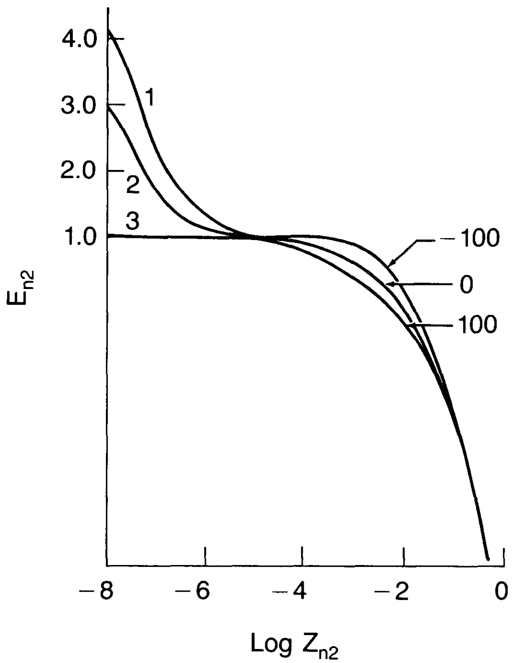

Fig. 4. Vertical profiles of dimensionless turbulent kinetic energy in the ocean at different dimensionless surface heat fluxes ($\mu = 0$, -100, 100) for various magnitudes of the wave parameter: (1) $C_1 = 20$; (2) $C_1 = 10$; (3) $C_1 = 0$.

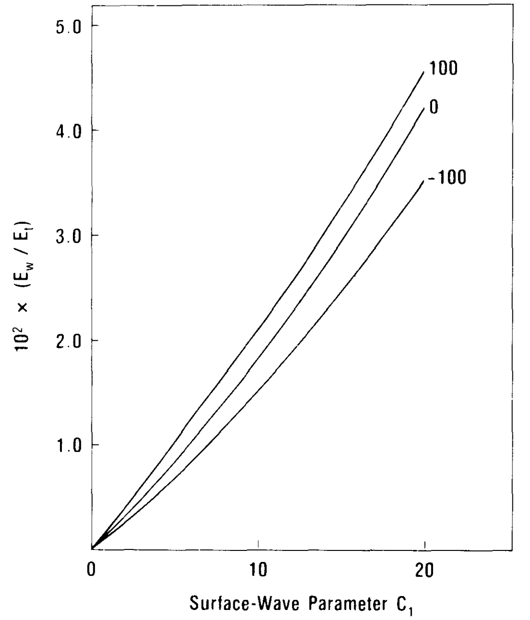

Fig. 5. Dependence of the ratio of the fraction of mean wind energy flux transferred to surface-wind waves (E_w) to total mean wind energy flux transferred from the atmosphere to the water (E_t) on the surface wave parameter C_1 for various dimensionless surface heat flux ($\mu = 0$, -100, 100) and geostrophic wind $U_g = 10$ m s^{-1}.

part of the turbulent layer in the ocean. There are no observed data on turbulent kinetic energy in the ocean.

Published results of dimensionless turbulent kinetic energy in the ocean $E_n|_{z_{0n}}$ (at the roughness length z_{02}) at magnitudes 3 and 4, corresponding to wave heights $h = 2.5$ m and $h = 3.5$ m, may be found in Tarnopolski and Shnaydman (1984). These wave heights correspond to wave parameter values $C_1 = 10$ and $C_1 = 20$, and the energy values agree well with the output of this model as shown in Fig. 4.

Fig. 5 shows the dependence of the ratio of mean wind energy flux transmitted by surface waves (E_w) to total mean wind energy flux transferred from the atmosphere to water (E_t) upon the surface-wave parameter (C_1) for various values of surface heat flux ($\mu = 100$, 0, -100). From the figure, we can see that the ratio (E_w/E_t) is only slightly dependent on the surface heat flux. For a magnitude of $C_1 = 20$, the ratio equals to 4.2×10^{-2} at neutral, 4.7×10^{-2} at stable and 3.5×10^{-2} at unstable conditions of the atmospheric surface layer. The effect of atmospheric stability on this ratio increases slightly with C_1. Based on the energy balance of surface-wind waves for different windspeeds and fetches, various investigators have given different estimates of the ratio (τ_w/τ_t) (varying between 10% and 40%) of the fraction of momentum flux spent in generating and maintaining gravity waves to the total momentum flux transmitted to the water (see Dubov, 1974; Kitaigorodski, 1973).

Plotted in Fig. 6 are the computed mean wind energy flux transmitted to surface waves (E_w) and to drift current (E_d) as a function of the surface-wave parameter C_1 for zero surface heat flux and geostrophic wind equal to 10 m s^{-1}. It is seen from the figure that E_d sharply decreases as C_1 is reduced below 15, and E_d moderately and weakly decreases for C_1 greater than 15. The decrease of E_d with increasing C_1 implies that more of the energy transferred to water by wind goes into generation and maintenance of surface waves and less towards generation of the drift current. At $C_1 = 5$ and 10, the magnitude of E_d decreases

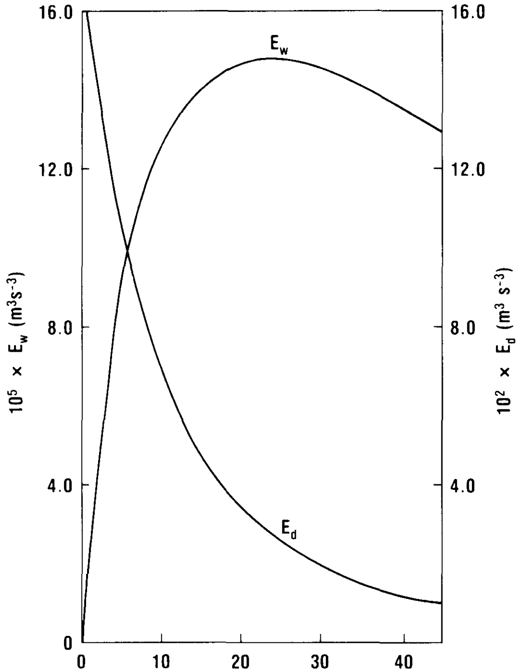

Fig. 6. Mean wind energy flux transmitted to surface waves (E_w) and to drift current (E_d) as a function of the surface-wave parameter C_1 for zero dimensionless surface heat flux ($\mu = 0$) and for the geostrophic wind $U_g = 10$ m s^{-1}.

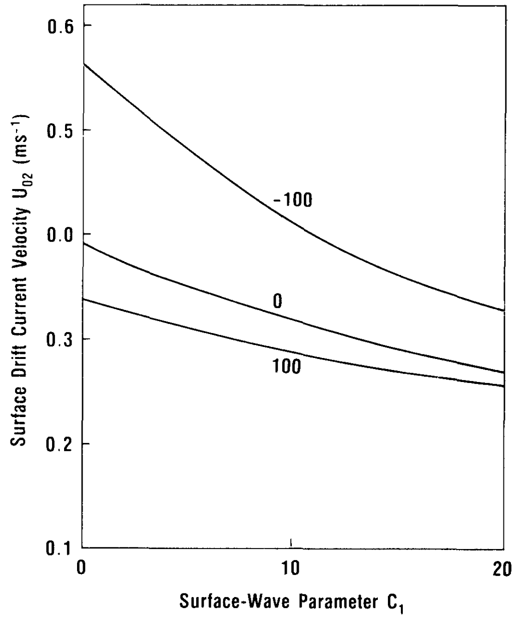

Fig. 7. Dependence of surface drift current velocity, U_{02}, on surface-wave parameter, C_1, at various dimensionless surface heat flux (zero, positive and negative) for the geostrophic wind $U_g = 15$ m s^{-1}.

over 30% and 50% respectively in comparison with E_d at $C_1 = 0$. This demonstrates the strong energetic connection between surface waves and drift current in the ocean.

It is seen also from Fig. 6 that E_w rapidly increases its magnitude for values of C_1 increasing from 0 to 20, reaches maximum at $C_1 = 20$, and then slowly decreases with increasing of C_1. At $C_1 = 20$, E_w reaches an equilibrium point. This equilibrium point probably related to saturation of the waves, and requires further study and direct experimental confirmation.

In Fig. 7 is shown the dependence of surface drift current on the surface-wave parameter C_1 for different surface heat fluxes (zero, positive and negative) at geostrophic wind equal to 15 m s^{-1}. The surface drift current, U_{02}, increases with increasing instability in the atmosphere (negative surface heat flux) as expected, because of more efficient downward transport of atmospheric momentum to the ocean surface. Negative dimensionless surface heat flux $\mu = -100$ increases the magnitudes of surface drift current roughly 33% and 22% in comparison with $\mu = 0$ for $C_1 = 0$ and $C = 10$, respectively. Positive non-dimensional surface heat flux $\mu = 100$ reduces the magnitude of surface drift current 15% and 12% in comparison with zero surface heat flux ($\mu = 0$) for $C_1 = 0$ and $C_1 = 10$, respectively. Surface drift current for the neutral atmosphere ($\mu = 0$) shrinks in magnitude about 20% and 30% for $C_1 = 10$ and $C_1 = 20$, respectively, when compared with the case for $C_1 = 0$. We can see from these results that a model of drift current in the ocean that neglects surface waves will overestimate the magnitude of the drift current (at least 20–30% for average waves).

4. Conclusions and remarks

In this study, the surface-wave effect, described by discontinuities of the turbulent kinetic energy flux and mean wind energy flux across the air–sea interface, is taken into account in a model for the planetary boundary layer over the ocean. The boundary conditions at the air–sea interface are obtained by means of a solution of the coupled model for air–sea boundary layers. A series of numerical experiments is carried out to determine the effects of surface waves on the structure of the upper turbulent layer in the ocean.

The results of the simulations show that surface waves reduce the neutral drag coefficient over the entire range of windspeeds. At $C_1 = 5$ (C_1 is a parameter representing the wave effect) the neutral drag coefficient matches well the observed data. Surface waves act as an additional source of turbulent kinetic energy for the upper part of the boundary layer in the ocean. Surface heat flux has virtually no effect on the distribution of turbulent kinetic energy in the ocean.

Numerical experiments confirm that the ratio of mean wind energy flux transferred to waves to total energy flux from the atmosphere is weakly affected by surface heat flux, and the part of the energy flux transmitted to drift current decreases rapidly with the increase of surface waves.

Computations also demonstrate that the surface drift current for the neutral atmosphere case decreases under surface-wave conditions when compared with the no-wave case, and is strongly affected by stability in the atmosphere.

The model results are in good agreement with the few available observational data on friction velocity and roughness lengths for $C_1 = 0$ conditions and on neutral drag coefficient for the wave conditions. The model agrees well with the accepted understanding of the influence of ocean surface waves and atmospheric stratification on the structure of air–sea coupled boundary layers.

It must be noted that the effect of surface waves on energy transfer at the air–sea interface is extremely complex and requires additional study. Further clarification will be achieved both by clearly describing the wave layer mathematically and by experimental investigations.

5. Acknowledgements

The author acknowledges the support of the Institute for Naval Oceanography. The Institute for Naval Oceanography is sponsored by the Navy and administered by University Corporation for Atmospheric Research. Computations were performed at the National Center for Atmospheric Research, which is supported by the National Science Foundation. The author is grateful to Dr. Altman at INO, Dr. Takle at ISU and Dr. Geernaert at NRL for their help and comments. This is the Institute for Naval Oceanography contribution no. 15.

REFERENCES

Charnock, H. 1955. Wind stress on a water surface. *Q. J. R. Meteorol. Soc. 81*, 639–640.

Deacon, E. L. and Webb, E. K. 1962. Interchange of properties between air and sea: Small scale interaction. In: *The sea, vol. 1* (ed. M. N. Hill). New York: Wiley-Interscience, 443–487.

Donelan, M. A. 1982. The dependence of aerodynamic drag coefficient on wave parameters. In: *Proceedings of the First International Conference on Meteorology and Coast Zone*. Boston, MA: Amer. Meteorol. Soc. 381–387.

Dubov, A. S. 1974. *Process of transfer near the air–sea interface*. Leningrad: Hydromet. Publ. House, 239 pp. (in Russian).

Francis, J. R. D. 1953. A note on the velocity distribution and bottom stress on a wind-driven water current system. *J. Mar. Res. 12*, 93–98.

Garratt, J. R. 1977. Review of drag coefficients over oceans and continents. *Mon. Wea. Rev. 105*, 915–929.

Geernaert, G. L., Katsaros, K. and Richer, K. 1986. Variation of the drag coefficient and its dependence on sea state. *J. Geophys. Res. 91*, 7667–7679.

Geernaert, G. L., Davidson, K. L., Larsen, S. E. and Mikkelsen, T. 1988. Wind stress measurements during the tower ocean wave and radar dependence experiment. *J. Geophys. Res. 93*, 13913–13923.

Goptarev, N. N. 1957. Some results of wind profile measurements in the Neftyanye Kamni Region. *Transac. State Oceanogr. Inst. 36* (in Russian).

Kamenkovich, V. M. and Monin, A. S. 1978. *The physics of ocean: hydrophysics of the ocean. Tom 1*, Moscow: "Nauka", 455 pp. (in Russian).

Kitaigorodski, S. A. 1973. *The physics of air–sea interaction*. Israel Prog. Scient. Transl. Jerusalem, 236 pp.

Klein, P. and Coantic, M. 1981. A numerical study of turbulent processes in the marine upper layers. *J. Phys. Oceanogr. 11*, 849–863.

Kundu, K. P. 1980. A numerical investigation of mixed-layer dynamics. *J. Phys. Oceanogr. 10*, 220–236.

Kuznetsov, O. A. 1963. The problem of aerodynamics roughness of the sea surface. *Transac. Inst. Oceangr. Acad. Sci. USSR, 72* (in Russian).

Kuznetsov, O. A. 1970. Results of an experimental investigation of the airflow over the sea surface. *Izv. Acad. Sci. USSR, Atmos. Oceanic Phys. 8*, 798–803 (in Russian).

Lai, R. J. and Shemdim, O. H. 1971. Laboratory investigation of air turbulence above simple water waves. *J. Geophys. Res. 30*, 7334–7350.

Large, W. G. and Pond, S. 1981. Open ocean momentum flux measurements in moderate to strong winds. *J. Phys. Oceanogr. 11*, 324–336.

Ly, N. L. 1981. On the parameterization of the oceanic atmospheric boundary layers. *Z. Meteor. 31*, 367–369.

Ly, N. L. 1986. Modeling the interaction between atmospheric and oceanic boundary layers, including a surface wave layer. *J. Phys. Oceanogr. 16*, 1430–1443.

Ly, N. L. 1989. An application of the pivotal-condensation method to modeling the air–sea boundary-layer structure. *Math. and Computer Modelling 9*, 1117–1130.

Ly, N. L. and Takle, E. S. 1988. A modeling study of the effects of baroclinicity on the structure of the interacting atmospheric and oceanic boundary layers. *J. Geophys. Res. 93*, 8203–8214.

Monin, A. S. 1986. *An introduction to the theory of climate.* Holland: Reidel Publish. Comp. 261 pp.

Monin, A. S. and Yaglom, A. M. 1971. *Statistical fluid mechanics: mechanisms of turbulence.* Cambridge: MIT Press, 769 pp.

Myers, V. A. 1959. Surface friction in a hurricane. *Mon. Wea. Rev. 8*, 307–311.

Neumann, G. 1956. Wind stress on water surface. *Bull. Amer. Meteorol. Soc. 5*, 211–217.

Roll, H. U. 1965. *Physics of the marine atmosphere.* New York/London: Academic Press, 426 pp.

Sheppard, P. A., Tribble, D. T. and Garratt, J. R. 1972. Studies of turbulence in the surface layer over water (Long Neath), I. Instrumentation, programme, and profiles. *Q. J. R. Meteorol. Soc. 98*, 627–641.

Smith, S. D. 1980. Wind stress and heat flux over the ocean in gale force winds. *J. Phys. Oceanogr. 19*, 709–726.

Smith, S. D. and Banke, E. G. 1975. Variations of the sea surface drag coefficient with wind speed. *Q. J. R. Meteorol. Soc. 101*, 665–673.

Tarnopolski, A. G. and Shnaydman, V. A. 1984. Modeling the interacting atmospheric and oceanic boundary layers. *Meteorol. and Hydrol. 5*, 48–56 (in Russian).

Tennekes, H. 1973. Similarity laws and scale relations in planetary boundary layer. In: *Workshop on micrometeorology* (ed. A. Haugen). Boston, MA: Amer. Meteor. Soc. 177–216.

Yeh, G. T. 1974. Interaction between the atmospheric and oceanic boundary layers. *Bound. Layer Meteor. 1*, 21–37.

Zilitinkevich, S. S. 1970. *Dynamics of the atmospheric boundary layer.* Leningrad: Hydromet. Publ. House, 290 pp. (in Russian).